Geoscience Frontiers 12 (2021) 219–230

HOSTED BY

Contents lists available at ScienceDirect

Geoscience Frontiers

journal homepage: www.elsevier.com/locate/gsf

Research Paper

Boron isotopic variations in tourmaline from metacarbonates and associated calc-silicate rocks from the Bohemian Massif: Constraints on boron recycling in the Variscan orogen

Lukáš Krmíček [a,b,c,*], Milan Novák [a], Robert B. Trumbull [d], Jan Cempírek [a], Stanislav Houzar [e]

[a] Department of Geological Sciences, Faculty of Science, Masaryk University, Kotlářská 2, CZ-611 37, Brno, Czech Republic
[b] Institute of Geology of the Czech Academy of Sciences, Rozvojová 269, CZ-165 02, Prague 6, Czech Republic
[c] Brno University of Technology, Faculty of Civil Engineering, AdMaS Centre, Veveří 95, CZ-602 00, Brno, Czech Republic
[d] GFZ German Research Centre for Geosciences, Telegrafenberg, D-14473, Potsdam, Germany
[e] Department of Mineralogy and Petrography, Moravian Museum, Zelný Trh 6, CZ-674 01, Brno, Czech Republic

ARTICLE INFO

Handling Editor: Kristoffer Szilas

Keywords:
Boron isotopes
Tourmaline
Metacarbonates
Moldanubicum
Variscan orogeny

ABSTRACT

Various metacarbonate and associated calc-silicate rocks form minor but genetically significant components of the lithological units in the Bohemian Massif of the Variscan orogen in Central Europe. These rocks vary in terms of their lithostratigraphy, chemical composition and mineral assemblage (dolomite/calcite ratio, silicate abundance). Tourmaline is present in five paragenetic settings within the metacarbonate and calc-silicate units. Type I comprises individual, euhedral, prismatic grains and grain aggregates in a carbonate-dominant (calcite ± dolomite) matrix poor in silicates. Type II is characterized by euhedral to subhedral grains and coarse- to fine-grained aggregates in silicate-rich layers/nests within metacarbonate bodies whereas type III occurs as prismatic grains and aggregates at the contact zones between carbonate and associated silicate host rocks. Type IV is in veins crosscutting metacarbonate bodies, and type V tourmaline occurs at the exocontacts of elbaite-subtype granitic pegmatite. Tourmaline from the different settings shows distinctive compositional features. Typical for type I are Mg-rich compositions, with fluor-uvite > dravite>> magnesio-lucchesiite. Tourmalines from type II silicate-rich layers/nests are highly variable, corresponding to oxy-schorl, magnesio-foitite, Al-rich dravite and fluor-uvite. Typical for type III tourmalines are Ca,Ti-bearing oxy-dravite compositions. The type IV veins feature dravite and fluor-uvite tourmaline compositions whereas type V tourmaline is Li,F-rich dravite. Tourmaline is the only B-bearing phase in paragenetic types I–IV, where it is characterised by two principal ranges of B-isotope composition ($\delta^{11}B = -13‰$ to $-9‰$ and $-18‰$ to $-14‰$). These ranges correspond to regionally different units of the Moldanubian Zone. Thus, the Svratka Unit (Moldanubian Zone s.l.) contains only isotopically lighter tourmaline ($\delta^{11}B = -18‰$ to $-14‰$), whereas metacarbonates in the Polička unit (Teplá–Barrandian Zone) and Olešnice unit (Moravicum of the Moravo-Silesian Zone) has exclusively isotopically heavier tourmaline ($\delta^{11}B = -9‰$ to $-13‰$). Tourmalines from metacarbonates in the Variegated Unit cover both ranges of isotope composition. The isotopically light end of the B isotope range may indicate the presence of continental evaporites within individual investigated areas. On the other hand, variations in the range of ~8 δ-units is consistent with the reported shift in B isotopic composition of metasedimentary rocks of the Bohemian Massif due to the prograde metamorphism from very-low grade to eclogite facies. In contrast to the metacarbonate-hosted settings, tourmaline of paragenetic type V from the exocontact of granitic pegmatites displays a significantly heavier range of $\delta^{11}B$ (as low as –7.7‰ to –0.6‰), which is attributed to partitioning of ^{10}B to cogenetic axinite and/or different B-signature of the source pegmatite containing tourmaline with heavy $\delta^{11}B$ signature.

* Corresponding author. Department of Geological Sciences, Faculty of Science, Masaryk University, Kotlářská 2, CZ-611 37, Brno, Czech Republic.
E-mail address: lukas.krmicek@gmail.com (L. Krmíček).
Peer-review under responsibility of China University of Geosciences (Beijing).

https://doi.org/10.1016/j.gsf.2020.03.009
Received 12 November 2019; Received in revised form 5 February 2020; Accepted 22 March 2020
Available online 1 April 2020

1. Introduction

Tourmaline is the dominant host for B in most rocks of the Earth crust, forming a minor to accessory mineral in granites and granitic pegmatites as well as in low-grade to ultra high-grade metamorphic rocks. Tourmaline is also present as a chemically and mechanically resistant detrital phase in sedimentary rocks and forms common gangue mineral in a wide range of hydrothermal deposits. Because of its stability and extremely low rates of volume diffusion for major and trace elements, tourmaline can retain chemical and textural information even at high P–T conditions (van Hinsberg et al., 2011). The combination of the wide stability range, highly variable chemical composition including B isotope ratios (e.g., Marschall and Jiang, 2011) and its refractory behaviour makes tourmaline a useful indicator of geological processes in igneous, hydrothermal, and metamorphosed systems (i.e., Dutrow and Henry, 2011 and references therein).

Tourmaline is a common mineral in many rock types but not in metacarbonates. Thus, there are few studies of the B-isotope composition of metacarbonate-hosted tourmaline but the available data show wide variations, suggesting a diversity of sources of boron in carbonate-dominant environment (van Hinsberg et al., 2011). Proposed sources include: (1) diagenetic or regional metamorphic alteration of original borate minerals, (2) hydrothermal fluids in areas underlain by continental evaporites such as in early rift basin settings, and (3) submarine fumarolic and hydrothermal activity independent of an evaporitic contribution (Warren, 2016 and references therein). While scenario (1) may pass to (2) as a continental rift basin evolves into a passive continental margin before being incorporated into a collisional orogen, scenario (3) can occur in volcanogenic rifts with or without the presence of evaporites. In terms of their major-element compositions, tourmalines from metaevaporite and/or metacarbonate environment are typically Ca–Mg-rich, intermediate between the end members dravite [$NaMg_3Al_6Si_6O_{18}(BO_3)_3(OH)_4$] and uvite [$Ca(Mg,Fe)_3MgAl_5Si_6O_{18}(BO_3)_3(OH)_4$] (Warren, 2016).

Tourmaline-bearing metacarbonates and associated calc-silicate rocks are widespread but minor components of the Bohemian Massif in the Czech Republic and neighboring countries (Houzar et al., 2017). Tourmaline in these rocks occurs as a scarce accessory phase (Povondra and Novák, 1986; Novák et al., 2003). Additionally, tourmaline commonly occurs as an accessory mineral in magmatic and clastic metasedimentary rocks from the Bohemian Massif, particularly in the Moldanubian Zone (Buriánek et al., 2017 and references therein) and the Svratka Unit (Čopjaková et al., 2009). Despite its scarcity, tourmaline composition can give important insights on the genesis of carbonate units in the Bohemian Massif. In this study we aim to (1) document the chemical and $^{10}B/^{11}B$ variability of tourmaline in a wide range of metacarbonate occurrences, (2) compare these with published data on tourmaline from the associated metasedimentary and granitic rocks to better understand the relationship of metacarbonates with their host

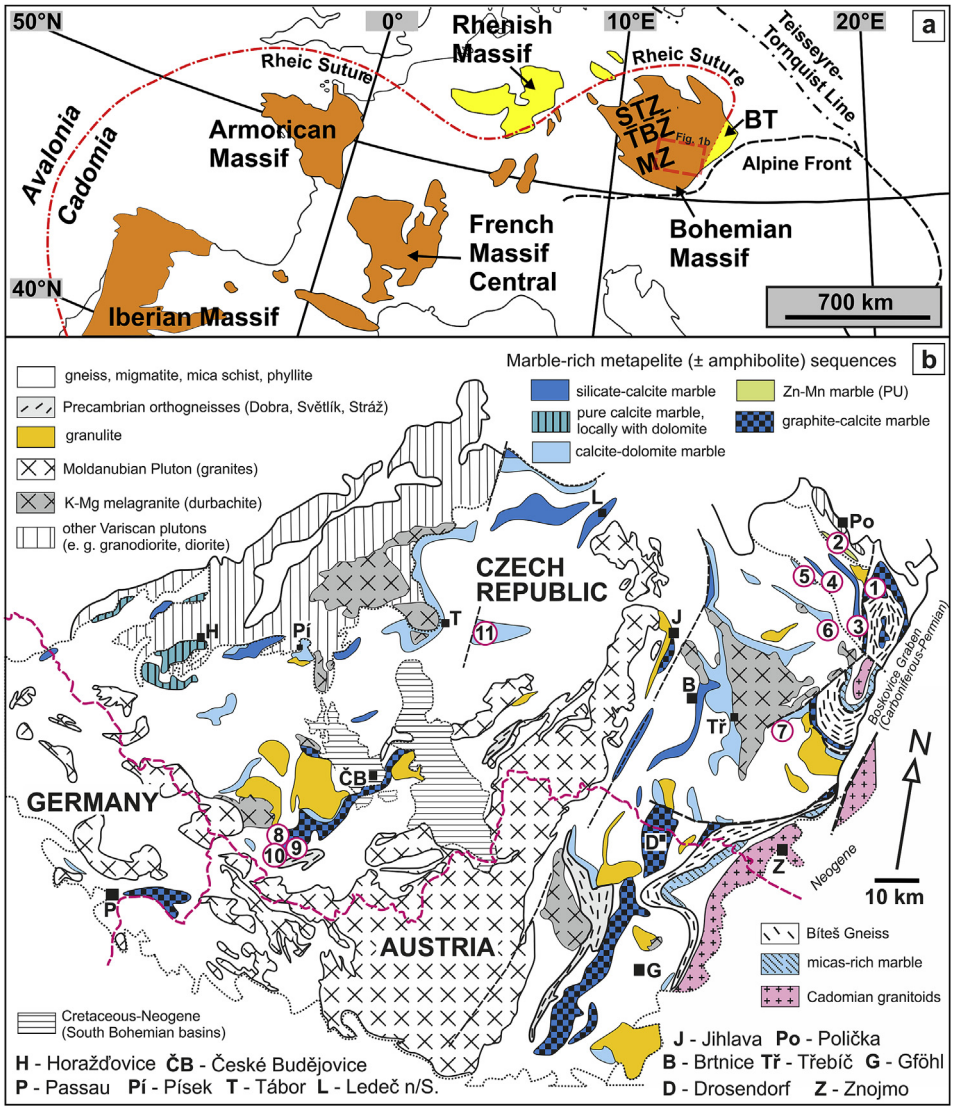

Fig. 1. (a) Location of the Rheic suture with respect to Cadomian and Variscan massifs in Western and Central Europe (after Krmíček et al., 2016 and references therein); (b) distribution of principal metacarbonates and calc-silicate rocks at eastern termination of the Moldanubian Zone and adjacent areas. Circles with numbers show the distribution of the studied tourmaline-bearing metacarbonates and associated calc-silicate rocks (see Table 1). Abbreviations: BT–Brunovistulian Terrane; MZ–Moldanubian Zone; STZ–Saxo-Thuringian Zone, and TBZ–Teplá–Barrandian Zone.

rocks, and (3) propose a scenario of boron sources in the metasedimentary protoliths and its behavior in the highly metamorphosed terrains such as the Bohemian Massif.

2. Geological setting and localities studied

The Bohemian Massif in Central Europe, which covers parts of Austria, the Czech Republic, Germany and Poland, includes blocks of continental Gondwana-related crust that were brought together during the Variscan orogeny (~370–300 Ma), when they collided with Laurussia. The collision zone is restricted to the eastern periphery of the Moldanubian Zone (Moldanubicum of Suess, 1926) and to the West Sudetes Domain (Lugicum of Suess, 1926) of the Saxo-Thuringian Zone of the European Variscides (*sensu* Kossmat, 1927; Fig. 1a). These units collided during the Variscan orogeny with the Cadomian (~600 Ma) Brunovistulian Terrane of the Moravo-Silesian Zone (e.g., Kalvoda et al., 2008; Timmerman et al., 2018a), forming a ca. 300 km long collision-related deformational belt ("Moravo-Silesicum" of Suess, 1926) with ophiolitic remnants of the Rheic Ocean (e.g., Krmíček et al., 2016). Increasing numbers of studies from the Bohemian Massif argue against the classical concept of several far-travelled blocks/terranes and favour the idea of a contiguous, vast Lower Palaeozoic Peri-Gondwanan shelf south of the Rheic Ocean (e.g., Kroner and Romer, 2013; Žák and Sláma, 2018; Stephan et al., 2019). Based on a recent zircon provenance study, the Peri-Gondwanan shelf was supplied by two super-fan systems from West Africa and East Africa–Arabia (Stephan et al., 2019).

Tourmalines from marbles and calc-silicate rocks occur in several regional units of the eastern part of Bohemian Massif, mostly in its highly-metamorphosed core: the Moldanubian Zone. This zone represents a crustal (and upper mantle) tectonic collage modified by several events of superimposed deformations and high- to low-grade metamorphic recrystallization. The rocks were intruded by numerous Carboniferous I-type to S-type granitic plutons. The Moldanubian architecture is defined by two principal lithotectonic units with distinct lithologies: (1) the Drosendorf Unit which comprises a structurally lowermost "Monotonous Group" of mainly migmatitic paragneisses intercalated with minor orthogneiss, quartzite, and amphibolite; and an overlying "Variegated Group" made up of paragneisses with abundant intercalations of amphibolite, marble, quartzite, graphite schist, and calc-silicate rocks. Structurally overlying the Drosendorf Unit is (2) the Gföhl Unit made up of felsic granulites, strongly serpentinized peridotites, eclogites and migmatitic orthogneisses (e.g., Matte et al., 1990; Finger et al., 2007; Guy et al., 2011; Schulmann et al., 2014).

Tourmaline-bearing metacarbonates and calc-silicate rocks are common but volumetrically minor (thickness typically <50 m) members of the Variegated Unit of the Moldanubian Zone (e.g., studied localities Blažkov, Třebenice, Studnice, Chýnov, Černá, Muckov, and Bližná) and in the adjacent metamorphic complexes that are genetically linked to the Kutná Hora-Svratka Complex (Moldanubicum s.l.), Teplá–Barrandian or Moravo-Silesian zones of the eastern Bohemian Massif (for characterisation of individual zones see McCann, 2008): the Nedvědice marbles from easternmost part of the Svratka Unit (at Nedvědice), central part of the Svratka Unit in the Dalečín region (at Písečné), the Trhonice marbles of the Polička Unit (at Sedliště) and the Olešnice Unit of the Moravicum (at Prosetín; Fig. 1b, Table 1). Based on mineral assemblages, the chemical composition of metacarbonates and the lithology of the host sequence several petrographic types were distinguished in previous studies (Novák, 1989; Houzar et al., 2017), as summarized in Table 1. (1) Silicate-rich calcite marbles (Qz + Di + Phl + An + Kfs + Tr + Ttn) - for abbreviations of mineral names see Whitney and Evans (2010) are common in lower sequences of the Variegated Unit typically interbedded with sillimanite-biotite paragneisses with intercalations of quartzites. (2) Silicate-poor calcite marbles (Phl + Di + Tr) locally with dolomite (<3–5 wt.% MgO) occur in all regions as nest-like bodies of different size. Additionally, large bodies, up to 300 m thick, of tourmaline-free, biogenic (reef-sourced) calcite marbles (Phl + Tr + Di), locally containing thin dolomite intercalations with Dol + Fo + Spl ± Chu occur in a monotonous complex of biotite paragneisses of the Sušice-Horaždovice

Table 1
Regional geological position and host rocks associations of metacarbonates and associated calc-silicate rocks from the investigated areas in the Bohemian Massif.

Zone/Unit	Region	Marble	Thickness m	Locality examined	Tur	Host rocks	Tourmaline/muscovite in host rock sequences				Ref.
							Metamorphic		Magmatic		
MSZ/Moravicum	Olešnice	Cal > Dol	<50	(1) Prosetín	A	Ms-Bt mica schist, graphite rocks, quartzite	Mica schist, metapegmatite	C/A	Pegmatite	N/A	1, 6, 9
TBZ/Polička Unit	Trhonice marble	Cal > Dol	<40	(2) Sedliště	R	Ms-Bt pearl gneiss, mica schist, amphibolite	Mica schist	R/C	Pegmatite	R/C	4
KHSC/Svratka Unit	Nedvědice marble	Cal	<40	(3) Nedvědice	R	Ms-Bt gneiss, mica schist	Orthogneiss, mica-schist, tourmalinite	A/A	Pegmatite	C/A	5
	Dalečín	Cal	<5	(4) Písečné	R	Ms-Bt gneiss	Mica-schist	R/A	Pegmatite	C/A	1, 10, 11
Moldanubicum	Strážek	Dol ≈ Cal	20–50	(5) Studnice	R	Bt-Sil gneiss, amphibolite	Orthogneiss	R/R	Pegmatite	C/C	1
				(6) Blažkov	A						
	Náměšť nad Oslavou	Dol ≈ Cal	<40	(7) Třebenice	A	Migmatite, amphibolite	Migmatite	R/N	Pegmatite, granite	C/C	
	Český Krumlov	Cal > Dol	30–70	(8) Černá	R	Bt-Sil gneiss, graphite rocks	Metapelite	R/R	Pegmatite, granite	C/R	3, 7, 9
				(9) Muckov	C						
				(10) Bližná	A						
	Chýnov	Dol ≈ Cal	<70	(11) Chýnov	C	Mica schist, amphibolite	Mica schists, orthogneiss	C/C	Pegmatite	R/C	2
	Ledeč nad Sázavou-Brtnice	Cal	<50	Not examined	N	Bt-Sil-Grt gneis, quartzite	Orthogneiss	N	Pegmatite	C/C	7
	Sušice-Horaždovice	Cal >> Dol	50–300	Not examined	N	Bt gneiss, migmatite		N	Pegmatite	C/C	7, 8

Abbreviations: MSZ – Moravo-Silesian Zone; TBZ – Teplá–Barrandian Zone; KHSC – Kutná Hora-Svratka Complex. Marble bodies are heterogeneous and both pure marbles and impure marbles with variable content of silicates occur within single marble body in all regions. Abundances of tourmaline/muscovite at the examined localities or in rocks from the host sequence: A – abundant, C – common to minor, R – rare, N – not found. Abundances of tourmaline (Tur) and muscovite are related to their obvious abundances in host rocks – accessory tourmaline and minor to major muscovite. References: 1 – Povondra and Novák (1986); 2 – Vrána et al. (1997); 3 – Novák et al. (1999); 4 – Novák et al. (2003); 5 – Houzar et al. (2006); 6 – Bačík et al. (2013); 7 – Houzar et al. (2017); 8 – Malecha et al. (1960); 9 – Kříbek (1997); 10 – Čopjaková et al. (2009); 11 – Buriánek et al. (2009).

region (Table 1). Elongated ductilly-deformed bodies of the Nedvědice marbles from the Svratka Unit enclosed in mica schists and two-mica gneisses with tourmaline orthogneisses have similar geological and compositional features. Blue calcite marble associated with Ca-skarns (Ves + Wo ± Grt, sulphides, native Bi, Sn- and B-rich accessory minerals; Houzar et al., 2006; Groat et al., 2013) are typical in the Nedvědice marbles. The Trhonice marbles (Ghn + Ba-Phl + Di + Amf + Hem) from the Polička Unit are similar in geology but distinct in composition, being enriched in Mn, Zn and Pb (Slobodník and Hladíková, 1994; Novák et al., 2003). (3) Graphite-rich banded marbles (Gr + Phl + Amf + Di ± Dol) form moderate to large bodies (<70 m) associated with graphitic rocks in mica schists and gneisses from the Olešnice and Český Krumlov units. The latter two regions differ solely in the degree of metamorphism (Table 1). (4) Intercalated layers of calcite and dolomite marbles (Fo + Chl + Amf + Spl ± Chu ± Di) in moderate to small bodies (<40 m thick) associated with numerous MORB-amphibolites in cordierite migmatites are typical for the contact of Variegated Unit with the overlaying Gföhl unit. (5) Pure dolomite (Fo + Spl + Phl), as rare small bodies, are present in metasedimentary lithologies enclosed in migmatite-orthogneiss of Gföhl type.

Metacarbonates and associated calc-silicate rocks contain tourmaline as a rare accessory mineral (Table 1, Fig. 2a–f). Tourmaline is more common in the Trhonice marbles (Sedliště) and at the locality Třebenice than elsewhere, but it is still an accessory mineral (Fig. 2d). Tourmaline is abundant only in Bližná, where a tourmaline + axinite reaction rim (10 cm thick) is locally developed in the footwall contact of the pegmatite and host marble (for details see Novák et al., 1999; Fig. 2f). Blue dravite in an albite-rich rock from the locality Prosetín (Bačík et al., 2012) is common (Table 1, Fig. 2b).

The lithologies hosting the tourmaline-bearing marbles and associated calc-silicate rocks differ significantly in abundance of tourmaline or other B-rich accessory minerals (Table 1). Tourmaline and other B-rich minerals are abundant in metamorphic rocks of the Svratka Unit (Čopjaková et al., 2009; Groat et al., 2013). In the Moldanubian Zone, orthogneiss is a typical tourmaline-bearing metamorphic rock (Vrána, 1997). Tourmaline is abundant in magmatic rocks – leucogranites (e.g., Buriánek and Novák, 2007) and locally abundant in various granitic pegmatites (e.g., Novák et al., 1999, 2011, 2012; Selway et al., 1999; Gadas et al., 2012). In other units/regions, tourmaline is rare. Moreover, the individual regional units differ significantly in abundance of muscovite/boromuscovite-bearing lithologies (Table 1).

3. Analytical methods

Chemical analyses of tourmaline (from cores and rim regions, up to 10 points per sample) were performed with the Cameca SX 100 electron microprobe at the Joint Laboratory of Electron Microscopy and Microanalysis (Department of Geological Sciences, Masaryk University, and Czech Geological Survey, Brno). Operating conditions for the wavelength-dispersive analyses involved an accelerating voltage of 15

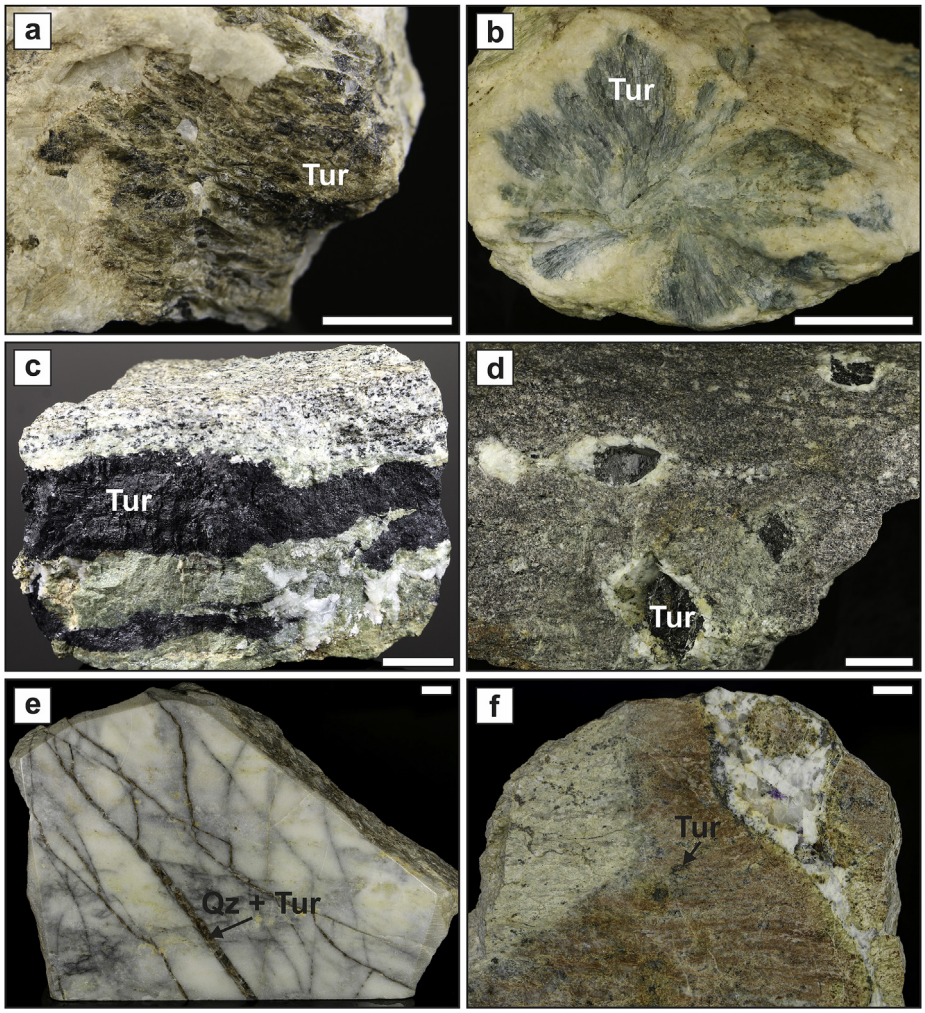

Fig. 2. Photographs of the investigated tourmaline-bearing metacarbonates and associated calc-silicate rocks from the Bohemian Massif: (a) Písečné (type I), (b) Prosetín (type II), (c) Nedvědice (type II), (d) Třebenice (type III), (e) Chýnov (type IV), (f) Bližná (type V). Scale bars are 1 cm long. For characteristics of individual types see text and Table 4. Tur = tourmaline, Qz = quartz.

kV, 10 nA beam current and a spot size ~5 μm. The following reference standards and X-ray Kα lines were used: sanidine (Si, Al, K), albite (Na), pyrope (Mg), titanite (Ti), chromite (Cr), vanadinite (Cl), fluorapatite (P), wollastonite (Ca), almandine (Fe), spessartine (Mn), $ScVO_4$ (V), gahnite (Zn), topaz (F) and ZnO (Zn). The peak counting times were 10–20 s for major and 20–40 s for minor elements. The background counting time was half that on the peak, on both the high- and low-energy positions. Standard deviations of individual elements vary from 1 to 10 rel.%, being the lowest for the main elements (Si, Al ~1 rel.%, Mg ~2 rel.%) and higher for minor elements (Ti ~4 rel.%, Ca, Fe ~6–7 rel.%, Na, F ~10 rel.%). Detection limits of the elements range from ca. 260 ppm (for Ti), through ~360 ppm (for Al, Mg, Ca), ~450 ppm (Si, Na), ~620 ppm (F) to ca. 750 ppm (Fe).

Crystal-chemical formulae of tourmaline were calculated assuming the general formula $XY_3Z_6T_6O_{18}(BO_3)_3V_3W$, where X = Na, Ca, K, vacancies; Y = Fe^{2+}, Mg, Mn, Ti, Al, Zn; Z = Al, Fe^{3+}, Mg; T = Si, Al; V = OH + O; W = OH + F + O (Henry et al., 2011). The formulae were normalized on the basis of T + Z + Y cations = 15 apfu; as most samples have Si close to 6 apfu (and only minor ^{T}Al), in few cases normalization on Si = 6 was used as it generates lower error in calculation of anions than excess charge from Si > 6 apfu. All Fe was assumed to be Fe^{2+} as no Fe^{3+} is required for charge balance and the mineral assemblages do not suggest oxidizing conditions. In data from Bližná sample, Li, B and H were calculated assuming Li = 15–(T + Z + Y), B = 3 apfu, and OH = 4–F; the calculated values are consistent with those measured by Novák et al. (1999). Tourmaline compositions and formulae are listed and discussed in atoms per formula unit (apfu). The coefficient X_{Mg} is defined as X_{Mg} = Mg/(Mg + Fe_{tot}). Compositions of tourmaline are summarized in Table 2.

Boron isotope analyses were conducted with the Cameca 1280-HR SIMS at the German Research Centre for Geosciences (GFZ) in Potsdam using the same mounts previously analyzed by electron microprobe. Back-scatter electron (BSE) images were used to select points for SIMS analyses. Prior to analysis, the samples were repolished to remove the carbon coating, cleaned in ethanol in an ultrasonic bath and coated with 35 nm of high-purity gold. The SIMS analyses employed a 4 nA, $^{16}O^-$ primary ion beam with an energy of 13 keV, focused to a diameter of about 5 μm on the sample surface. Positive secondary ions were extracted using a 10 kV potential, with no offset voltage applied. Each analysis was preceded by a 90-s pre-sputtering to remove the gold coat and establish stable sputter conditions. The analyses were done in multicollection mode with faraday cups, each consisting of 20 cycles with 4 s integration time per cycle. The mass resolution of the instrument was M/ΔM ≈ 2000, which is more than adequate to separate the $^{11}B^+$ and $^{10}B^1H^+$ mass stations. The typical count rate for $^{11}B^+$ under these conditions was about 1.5 × 107 ions per second. Correction for instrumental mass fractionation (IMF) and monitoring analytical quality were done with multiple analyses of tourmaline reference materials dravite (#108796) and schorl (#112566) from the Harvard Mineralogical Museum (Dyar et al., 2001). Individual uncertainties on 20 cycles are reported in Table 3. Analytical repeatability on individual reference materials was <0.2‰ (Table 3). The variability for all analyses from both reference materials was <0.8‰ (1 SD, n = 50), which includes any chemical matrix effect and is our estimate for the overall reliability of the data. After correction for the mean value of IMF for all reference materials, the measured $^{11}B/^{10}B$ ratios were converted to $\delta^{11}B$ values relative to the NBS SRM-951 value of 4.04362 (Catanzaro et al., 1970). Boron isotopic variations in tourmaline are given in Supplement A in the electronic appendix to this paper and summarized in Table 4.

4. Results

4.1. Paragenetic types of tourmaline

Five distinctive paragenetic types (type I–V) of tourmaline are recognized in this study (Table 4) based on different textural and paragenetic positions of tourmaline within the investigated metacarbonates and calc-silicate rocks. **Paragenetic type I** involves individual, euhedral, prismatic grains and grain aggregates up to 3 cm long, enclosed in low content of silicates (pure marble to slightly impure, silicates-enriched marble) in a calcite ± dolomite marble with rare silicate-enriched domains containing minor phlogopite, diopside, chlorite and/or quartz. **Type II** comprises euhedral to subhedral tourmaline grains up to 5 cm in length, and coarse- to fine-grained aggregates in calc-silicate layers or nests within the metacarbonate bodies. This tourmaline is associated with albite, oligoclase, diopside, K-feldspar, chlorite and/or margarite. The host rock varies from massive calc-silicate rock (several cm in size) with <5 vol% carbonate (Nedvědice, Prosetín) to thin silicate-rich layer (≤5 mm) in pure marble (Studnice). **Paragenetic type III** tourmaline forms prismatic grains and grain aggregates up to 5 cm in size, in calc-silicate contact zones between the metacarbonate and associated host silicate rocks. The latter are highly variable in lithology and mineral assemblage. They include: amphibolite (amphibole, epidote, plagioclase, titanite), and migmatized biotite gneiss with scapolite, diopside, titanite, epidote and humite-group minerals. **Paragenetic type IV** comprises tourmaline in quartz- or diopside-tremolite veins crosscutting metacarbonate. Finally, **paragenetic type V** occurs in a reaction zone between an elbaite-subtype granitic pegmatite and host impure marble. This zone, about 10 cm thick and 1 m long, is made up of dominant tourmaline, axinite, and minor pyrite and fluorite (see also Novák et al., 1999).

4.2. Chemical composition of tourmalines

The backscattered-electron imaging revealed several different styles of internal variations in tourmaline grains from the different paragenetic types. These include homogeneous grains, locally with Fe-rich overgrowths, to heterogeneous grains with more or less perfectly developed fine oscillatory zoning. The rare presence of late veining and/or patchy zonation was also observed locally (Fig. 3a–h). Despite the observed textural zoning, the tourmalines typically have relatively homogeneous composition, with exception of the sample from Studnice with Mg-rich crystal cores and Fe-rich rims (Fig. 4).

Paragenetic type I: Tourmalines hosted in marbles classify, in decreasing abundance, as fluor-uvite > dravite >> magnesio-lucchesiite. They are characterized by large variations in Ca contents and low X-site vacancies (Fig. 4). Tourmaline from the localities Písečné, Černá and Sedliště display distinct ranges in X_{Mg} of 0.68–0.97, 0.57–0.61, 0.32–0.34, respectively, with overall 0.00–0.14 apfu F (Table 2).

Paragenetic type II: Tourmalines from silicate-rich layers/nests comprise oxy-schorl to magnesio-foitite, Al-rich dravite and fluor-uvite compositions. They are similar to type I tourmalines but with large variation in Ca contents and low X-site vacancies (Fig. 4). Dravite from Prosetín is particularly Ca-poor compared with other localities (Table 2; Bačík et al., 2012). There are also distinctive variations for the individual localities Studnice, Nedvědice and Prosetín, in terms X_{Mg} (0.28–0.64, 0.64–0.66 and 0.88–0.90 respectively) and F (0.03–0.08, 0.50–0.53 and 0.02–0.05 apfu respectively). Tourmaline from Studnice is also particularly Al-rich with ~7.0 apfu Al_{tot}.

Paragenetic type III: Tourmaline from contact zones corresponds to a Ca,Ti-bearing oxy-dravite, with moderate variation in Ca contents, low X-site vacancies and low F contents ≤0.1 apfu (Fig. 4). Minor differences in X_{Mg} were found for the individual localities Blažkov, and Třebenice. The contents of Ti range from 0.07 to 0.17 apfu. Both Mn and Zn are below or close to the detection limits in all samples except for Nedvědice tourmaline with up to 0.28 wt.% ZnO (Table 2).

Paragenetic type IV: Tourmaline from veins in both localities Muckov and Chýnov has very high and constant X_{Mg} ratios (0.96–0.97 and 0.91–0.92, respectively). The Muckov tourmaline is fluor-uvite characterized by high Ca (0.75–0.83 apfu), F (0.69–0.81 apfu) and low Al_{tot} (5.35–5.59 apfu), whereas the Chýnov veins contain dravite

Table 2
Representative analyses of tourmaline from the investigated areas in the Bohemian Massif.

	Písečné (type I)		Sedliště (type I)		Černá (type I)		Nedvědice (type II)		Prosetín (type II)		Studnice (type II)		Blažkov (type III)		Třebenice (type III)		Muckov (type IV)		Chýnov (type IV)		Bližná (type V)	
SiO_2	35.99	36.91	36.95	35.95	35.81	36.44	35.12	35.51	37.48	37.55	36.13	33.35	36.48	36.87	35.00	34.84	36.64	37.09	37.40	37.79	37.32	37.47
TiO_2	0.28	0.27	0.10	0.71	1.62	1.58	0.34	0.33	0.00	0.00	0.01	0.57	0.57	0.90	0.93	0.95	0.18	0.30	0.73	0.27	0.09	2.46
Al_2O_3	28.69	28.89	32.87	29.60	28.81	29.06	28.88	28.87	35.07	35.88	36.00	35.83	33.58	32.78	32.85	33.06	29.41	28.35	32.62	34.13	33.02	28.72
V_2O_3	0.04	0.00	0.02	0.00	0.07	0.09	0.03	0.05	0.01	0.03	0.00	0.06	0.00	0.00	0.00	0.00	0.02	0.00	0.10	0.07	0.00	0.00
Cr_2O_3	0.00	0.00	0.00	0.01	0.08	0.07	0.01	0.00	0.00	0.00	0.00	0.00	0.00	0.07	0.06	0.00	0.00	0.02	0.02	0.03	0.00	0.00
FeO	0.70	0.77	4.75	7.36	2.15	2.09	8.30	8.62	1.91	2.26	5.36	11.38	3.54	3.77	6.34	6.17	0.91	0.86	1.94	1.69	0.90	2.44
MnO	0.03	0.02	0.03	0.01	0.03	0.02	0.09	0.07	0.02	0.01	0.00	0.08	0.00	0.00	0.00	0.00	0.01	0.01	0.02	0.00	0.25	0.18
ZnO	0.01	0.00	0.04	0.06	0.00	0.00	0.27	0.25	0.00	0.05	0.02	0.06	0.00	0.00	0.00	0.00	0.01	0.07	0.06	0.04	0.00	0.00
MgO	14.54	14.05	9.05	8.98	12.13	12.20	8.62	8.69	9.33	8.68	5.36	2.45	8.59	8.64	7.21	7.10	14.44	14.81	10.99	9.75	10.70	11.80
CaO	4.79	4.38	0.86	2.12	3.75	3.66	3.22	2.98	0.41	0.29	0.75	1.20	1.33	1.55	2.15	2.05	4.57	4.83	0.97	0.50	0.70	1.27
Na_2O	0.72	0.81	2.04	1.85	1.11	1.14	1.41	1.42	2.40	2.16	1.23	1.19	1.93	2.13	1.69	2.03	0.67	0.49	2.45	2.63	2.60	2.35
K_2O	0.00	0.00	0.03	0.02	0.04	0.03	0.05	0.07	0.03	0.01	0.01	0.06	0.05	0.00	0.10	0.12	0.00	0.02	0.01	0.01	0.00	0.00
F	1.18	1.13	0.05	0.27	0.66	0.66	0.94	0.99	0.06	0.09	0.09	0.08	0.13	0.15	0.11	0.11	1.61	1.56	0.37	0.10	0.35	0.90
B_2O_3[a]	10.70	10.75	10.81	10.54	10.54	10.66	10.37	10.46	10.93	10.98	10.55	10.35	10.69	10.69	10.49	10.46	10.86	10.85	10.95	10.95	10.91	10.88
Li_2O[a]	–	–	–	–	–	–	–	–	–	–	–	–	–	–	–	–	–	–	–	–	0.24	0.22
H_2O[a]	2.99	2.91	3.63	3.39	2.86	2.88	2.96	3.06	3.39	3.41	3.09	3.29	3.15	2.96	3.04	2.93	2.90	2.88	3.38	3.37	3.60	3.32
–(O=F)	−0.50	−0.48	−0.02	−0.11	−0.28	−0.28	−0.40	−0.42	−0.03	−0.04	−0.04	−0.03	−0.05	−0.06	−0.05	−0.04	−0.68	−0.66	−0.15	−0.04	−0.15	−0.38
Total	100.16	100.41	101.21	100.76	99.38	100.3	100.21	100.95	101.01	101.36	98.56	99.92	99.99	100.45	99.92	99.78	101.55	101.48	101.86	101.29	100.53	101.63
^{T}Si	5.846	5.969	5.942	5.928	5.902	5.944	5.885	5.902	5.959	5.946	5.952	5.600	5.931	5.994	5.801	5.789	5.862	5.944	5.934	6.000	5.945	5.989
^{T}Al	0.154	0.031	0.058	0.072	0.098	0.056	0.115	0.098	0.041	0.054	0.048	0.400	0.069	0.006	0.199	0.211	0.138	0.056	0.066	0.000	0.055	0.011
B	3.000	3.000	3.000	3.000	3.000	3.000	3.000	3.000	3.000	3.000	3.000	3.000	3.000	3.000	3.000	3.000	3.000	3.000	3.000	3.000	3.000	3.000
^{Z}Al	5.338	5.475	6.000	5.681	5.499	5.531	5.589	5.558	6.000	6.000	6.000	6.000	6.000	6.000	6.000	6.000	5.409	5.299	6.000	6.000	6.000	5.399
^{Z}Mg	0.662	0.525	0.000	0.319	0.501	0.469	0.411	0.442	0.000	0.000	0.000	0.000	0.000	0.000	0.000	0.000	0.591	0.701	0.000	0.000	0.000	0.601
^{Y}Ti	0.035	0.032	0.012	0.087	0.200	0.194	0.043	0.042	0.000	0.000	0.001	0.071	0.070	0.111	0.115	0.119	0.021	0.036	0.087	0.033	0.011	0.296
^{Y}Al	0.000	0.000	0.171	0.000	0.000	0.000	0.000	0.000	0.531	0.641	0.942	0.690	0.367	0.275	0.217	0.265	0.000	0.000	0.033	0.386	0.144	0.000
^{Y}V	0.005	0.000	0.003	0.000	0.010	0.012	0.005	0.007	0.001	0.003	0.000	0.008	0.000	0.000	0.000	0.000	0.002	0.000	0.012	0.009	0.000	0.000
^{Y}Cr	0.000	0.000	0.000	0.001	0.010	0.009	0.001	0.000	0.000	0.000	0.000	0.000	0.000	0.009	0.007	0.000	0.000	0.003	0.002	0.004	0.000	0.000
$^{Y}Fe^{2+}$	0.095	0.104	0.638	1.015	0.297	0.285	1.163	1.198	0.254	0.299	0.739	1.599	0.481	0.512	0.879	0.858	0.122	0.115	0.257	0.224	0.120	0.325
^{Y}Mn	0.004	0.003	0.004	0.002	0.004	0.003	0.013	0.010	0.002	0.001	0.000	0.011	0.000	0.000	0.000	0.000	0.001	0.001	0.003	0.000	0.033	0.024
^{Y}Zn	0.001	0.000	0.004	0.008	0.000	0.000	0.034	0.031	0.000	0.006	0.002	0.008	0.000	0.000	0.000	0.000	0.002	0.008	0.007	0.005	0.000	0.000
^{Y}Mg	2.860	2.861	2.168	1.888	2.480	2.497	1.742	1.712	2.212	2.049	1.316	0.613	2.083	2.094	1.782	1.758	2.852	2.837	2.598	2.308	2.541	2.211
^{Y}Li	–	–	–	–	–	–	–	–	–	–	–	–	–	–	–	–	–	–	–	–	0.152	0.143
^{X}Ca	0.834	0.759	0.148	0.375	0.663	0.639	0.579	0.531	0.069	0.049	0.133	0.215	0.232	0.271	0.381	0.365	0.784	0.829	0.165	0.086	0.120	0.217
^{X}Na	0.227	0.255	0.635	0.593	0.354	0.359	0.457	0.458	0.738	0.662	0.394	0.388	0.609	0.672	0.544	0.654	0.208	0.152	0.753	0.811	0.802	0.729
^{X}K	0.001	0.000	0.005	0.004	0.007	0.006	0.011	0.016	0.006	0.002	0.003	0.012	0.010	0.000	0.020	0.026	0.001	0.004	0.002	0.002	0.000	0.000
^{X}vac	0.000	0.000	0.212	0.029	0.000	0.000	0.000	0.000	0.187	0.287	0.471	0.384	0.148	0.057	0.055	0.000	0.008	0.015	0.080	0.101	0.078	0.054
^{V}OH	3.000	3.000	3.000	3.000	3.000	3.000	3.000	3.000	3.000	3.000	3.000	3.000	3.000	3.000	3.000	3.000	3.000	3.000	3.000	3.000	3.000	3.000
^{W}F	0.605	0.579	0.026	0.141	0.343	0.339	0.499	0.519	0.032	0.046	0.046	0.044	0.064	0.075	0.058	0.055	0.813	0.792	0.185	0.048	0.174	0.456
^{W}OH	0.240	0.137	0.897	0.729	0.145	0.133	0.308	0.395	0.593	0.603	0.396	0.685	0.415	0.213	0.361	0.242	0.096	0.076	0.576	0.566	0.826	0.544
^{W}O	0.155	0.281	0.076	0.130	0.508	0.528	0.192	0.086	0.374	0.352	0.558	0.272	0.521	0.712	0.582	0.702	0.091	0.132	0.240	0.385	0.000	0.000

[a] Calculated assuming B = 3 apfu, OH = 31−O−F, and Li = 15−(T + Z + Y). Li_2O determined by ion microprobe (Novák et al., 1999).

Table 3
Results of SIMS B-isotope analyses on reference tourmalines.

Analysis date	$^{11}B/^{10}B$	1 SD (‰)[a]	IMF[b]	$^{11}B/^{10}B_{corr}$	$\delta^{11}B$ (‰)[c]
Schorl ($^{11}B/^{10}B$ = 3.993 and $\delta^{11}B$ = −12.5‰)					
02/27/2017	3.909	0.16	0.9788	3.996	−11.7
02/27/2017	3.908	0.32	0.9788	3.996	−11.7
02/27/2017	3.910	0.24	0.9792	3.997	−11.3
02/27/2017	3.909	0.21	0.9789	3.996	−11.6
02/27/2017	3.909	0.27	0.9790	3.997	−11.5
02/27/2017	3.909	0.21	0.9789	3.996	−11.6
02/27/2017	3.911	0.22	0.9794	3.998	−11.1
02/27/2017	3.909	0.20	0.9789	3.996	−11.6
02/27/2017	3.909	0.24	0.9788	3.996	−11.7
02/27/2017	3.908	0.21	0.9787	3.995	−11.8
02/27/2017	3.908	0.20	0.9787	3.996	−11.8
02/27/2017	3.908	0.22	0.9787	3.995	−11.8
02/27/2017	3.908	0.23	0.9787	3.996	−11.8
02/27/2017	3.909	0.26	0.9789	3.996	−11.6
02/27/2017	3.908	0.22	0.9787	3.996	−11.8
02/28/2017	3.908	0.30	0.9788	3.997	−11.7
02/28/2017	3.908	0.21	0.9787	3.996	−11.8
02/28/2017	3.909	0.27	0.9789	3.997	−11.6
02/28/2017	3.908	0.30	0.9786	3.996	−11.9
02/28/2017	3.908	0.24	0.9786	3.996	−11.9
02/28/2017	3.907	0.24	0.9786	3.996	−11.9
02/28/2017	3.908	0.25	0.9787	3.997	−11.8
02/28/2017	3.907	0.33	0.9784	3.995	−12.1
02/28/2017	3.908	0.29	0.9787	3.996	−11.8
02/28/2017	3.908	0.21	0.9787	3.996	−11.8
02/28/2017	3.908	0.29	0.9786	3.996	−11.9
Mean	3.908				−11.7
Repeatability in ‰[d]	0.19				
Dravite ($^{11}B/^{10}B$ = 4.017 and $\delta^{11}B$ = −6.6‰)					
02/27/2017	3.925	0.35	0.9772	4.013	−7.4
02/27/2017	3.926	0.31	0.9773	4.013	−7.3
02/27/2017	3.925	0.30	0.9771	4.013	−7.5
02/27/2017	3.926	0.28	0.9774	4.014	−7.2
02/27/2017	3.925	0.17	0.9772	4.013	−7.4
02/27/2017	3.926	0.23	0.9775	4.014	−7.1
02/27/2017	3.926	0.33	0.9773	4.013	−7.3
02/27/2017	3.927	0.26	0.9775	4.014	−7.1
02/27/2017	3.926	0.25	0.9773	4.014	−7.3
02/27/2017	3.925	0.21	0.9770	4.012	−7.6
02/27/2017	3.925	0.26	0.9772	4.013	−7.4
02/27/2017	3.925	0.24	0.9771	4.013	−7.5
02/27/2017	3.925	0.31	0.9772	4.013	−7.4
02/28/2017	3.925	0.31	0.9772	4.014	−7.4
02/28/2017	3.924	0.22	0.9768	4.013	−7.8
02/28/2017	3.925	0.29	0.9770	4.014	−7.6
02/28/2017	3.925	0.20	0.9770	4.013	−7.6
02/28/2017	3.925	0.25	0.9772	4.014	−7.4
02/28/2017	3.924	0.25	0.9769	4.013	−7.8
02/28/2017	3.925	0.29	0.9772	4.014	−7.4
02/28/2017	3.925	0.24	0.9771	4.014	−7.5
02/28/2017	3.924	0.22	0.9769	4.013	−7.7
02/28/2017	3.925	0.33	0.9772	4.014	−7.4
02/28/2017	3.924	0.19	0.9770	4.013	−7.7
Mean	3.925				−7.5
Repeatability in ‰[d]	0.18				

[a] Individual uncertainty for 100 cycles (standard deviation/mean) × 1000.
[b] Instrumental mass fractionation ($^{11}B/^{10}B_{measured}$)/($^{11}B/^{10}B_{reference\ material}$).
[c] Calculated $^{11}B/^{10}B$ = 4.04362 for NBS SRM 951 from ratios corrected with average IMF values of 0.9780.
[d] Repeatability (standard deviation/mean) × 1000 in permil from multiple analyses of each reference material.

with high Na (0.67–0.81 apfu), low F (0.02–0.18 apfu), and high Al (6.10–6.44 apfu) (Table 2).

Paragenetic type V: Tourmaline from the exocontact of the Bližná pegmatite is a Li,F-rich dravite, unique by its elevated Li contents (up to 0.28 apfu according to ion microprobe data in Novák et al., 1999). Despite the Ca-rich assemblage of the contact zone, tourmaline has high Na (0.70–0.87 apfu) and low Ca (0.12–0.22 apfu), and features highly variable F (0.05–0.46 apfu), Al (5.35–6.20 apfu), and high X_{Mg} (0.90–0.96).

Table 4
Summary of tourmaline paragenetic types, principal mineral assemblages and range of boron isotopic composition in metacarbonates (I) and associated calc-silicate rocks (II, III, IV, V) from the Bohemian Massif.

Geological unit/Locality	Paragenetic type[a]	Tourmaline	Assemblage	$\delta^{11}B$ (‰)[b]
Variegated Unit				
Blažkov	III	Ca,Ti-bearing oxy-dravite	Pl, Sc, Ttn, Di, Ep	−14.4 to −15.2
Třebenice	III	Ca,Ti-bearing oxy-dravite	Ttn, Ep, Phl	−12.1 to −12.8
Studnice	II	oxy-schorl, magnesio-foitite	Phl, Ms	−9.3 to −10.6
Chýnov	IV	dravite	Qz	−16.7 to −18.1
Muckov	IV	fluor-uvite	Di, Phl	−11.2 to −11.5
Černá	I	fluor-uvite to Mg-lucchesiite	Cal, Pl, Ap	−11.6
Bližná	V	Li,F-rich dravite	Ax, Qz, Py, Fl	−0.6 to −7.7
Svratka Unit				
Nedvědice	II	fluor-uvite	Kfs, Di	−14.6 to −15.6
Písečné	I	fluor-uvite	Cal, Qz, Kf, Di	−15.6 to −17.5 −13.2 (“altered” marginal parts)
Polička Unit				
Sedliště	I	dravite	Cal, Phl, Di	−10.9 to −11.6
Moravicum				
Prosetín	II	Al-rich dravite	Ab, Ttn	−10.5 to −11.1

[a] For the detailed description of paragenetic types see text.
[b] For complete dataset of boron isotopic variations see Supplement S1.

4.3. Boron isotopic compositions

The studied samples from paragenetic types I–IV are characterized by two principal $\delta^{11}B$ signatures: (1) a relatively heavier isotope signature with an overall range from −13‰ to −9‰ and (2) a relatively lighter isotope signature characterised by an overall range from −18‰ to −14‰ (Table 4; Fig. 5). Tourmaline crystals show negligible or weak B-isotope zoning, with a maximum range of 3 δ-units. An exception to this homogeneity is tourmaline of type I from Písečné, which shows an “altered” zone in BSE image along fractures (Fig. 3a). This zone is ~5 δ-units lighter in B-isotope composition compared to other parts of the same grain.

Tourmaline from paragenetic type V (locality Bližná) significantly differs from tourmaline from other paragenetic types by heavier $\delta^{11}B$ values in the range of –7.7‰ to –0.6‰. It is similar in isotope composition to tourmaline from adjacent pegmatites, which have $\delta^{11}B$ values between –4.9‰ and –3.6‰ (unpublished data of M. Novák; Fig. 5).

From a regional point of view, the Variegated Unit of the Moldanubian Zone hosts metacarbonates containing tourmaline with two ranges of B-isotope ratios. The Svratka Unit hosts only tourmaline with isotopically lighter $\delta^{11}B$ signatures, whereas tourmaline from metacarbonates in the adjacent Polička and Olešnice units displays exclusively isotopically heavier $\delta^{11}B$ signatures (Fig. 5).

5. Discussion

5.1. Paragenetic setting and chemical composition of tourmaline

In general, chemical analyses of tourmaline from marbles and calc-silicate rocks are scarce in the literature, and comparisons are therefore limited. The composition of tourmaline types I to III in this study is similar to what has been described by other workers (e.g., Grice and Ercit, 1993; Deer et al., 1997; Dyar et al., 1998). The five paragenetic types of tourmaline described above have some distinctive compositional features. Uvite > fluor-uvite > dravite > magnesio-lucchesiite with high X_{Mg} and low Al_{tot} are typical for the type (I) marble-hosted tourmaline. Tourmalines

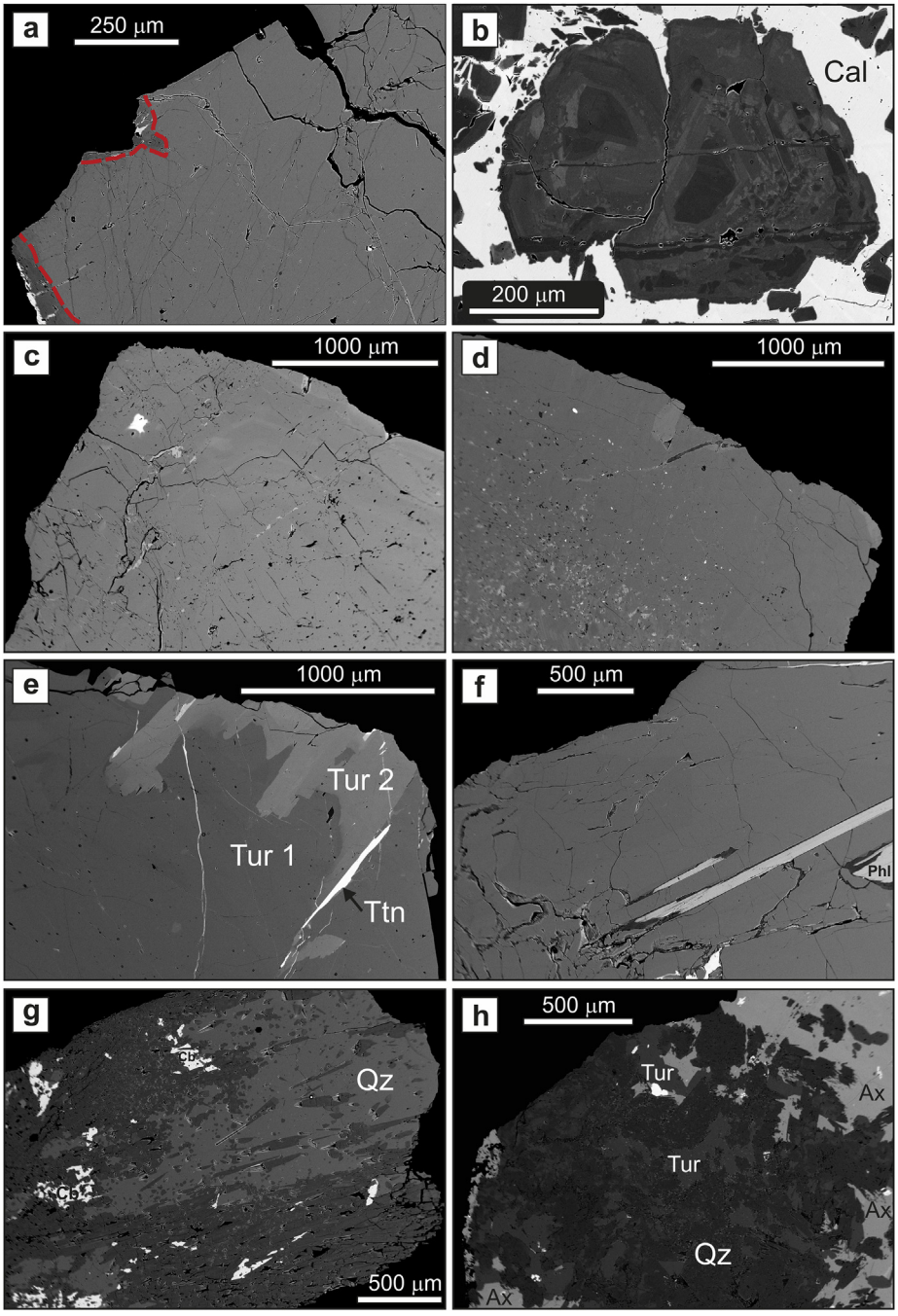

Fig. 3. Backscatter electron images of the investigated tourmaline samples: (a) tourmaline showing darker "altered" parts highlighted with a red dashed line (Písečné; type I); (b) tourmaline with intensively oscillatory zoning in a calcite (Cal) matrix; although tourmaline is intensively zoned, we did not find any replacement textures and tourmaline seems to be in equilibrium with other minerals (Sedliště; type I); (c) compositionally homogeneous tourmaline (Nedvědice; type II); (d) compositionally homogeneous tourmaline (Blažkov; type III); (e) early tourmaline (Tur 1) with Fe-rich overgrowths (Tur 2) and inclusion of acicular titanite (Ttn) (Třebenice; type III); (f) homogeneous tourmaline enclosing phlogopite (Phl) flakes (Muckov; type IV); (g) tourmaline aggregates in quartz (Qz)–carbonate (Cb)–tourmaline-bearing veins cutting host marble (Chýnov; type IV); (h) intergrown quartz–tourmaline–axinite from contact zone between marble and pegmatite (Bližná; type V). Zoned tourmaline in Fig. 3b is paragenetic type I from pure or almost pure marble with low amount of silicates and we did not find any replacement textures to associated silicates but they are not in a direct contact. It is likely in equilibrium with other minerals. Zoned tourmaline in Fig. 3e – we did not found inclusions of carbonates in tourmalines except for Chýnov, paragenetic type IV.

from (II) silicates-rich layers/nests, and (III) contact zones are more variable including (II) schorl, foitite, dravite, fluor-uvite and (III) dravite, oxy-dravite, respectively. Tourmalines from (IV) cross-cutting veins in low-T (Chýnov) and moderate-T (Muckov) are both Mg-rich but differ significantly in concentrations Ca and F (low-F dravite vs. fluor-uvite). Tourmaline from exocontact in Bližná (elbaite pegmatite Bližná I; Novák et al., 1999) (paragenetic type V) is associated with axinite and differs significantly in its chemical composition. It is Al-rich and contains elevated content of Li, what may be indicative for genetic connection with fluids exsolved from the adjacent pegmatite (see also Section 5.3.3).

The abundance of tourmaline in the host rocks differs significantly (Table 1). Tourmaline is mostly an accessory mineral at all paragenetic types. Among the metacarbonate rocks, tourmaline is most common in the Sedliště, Třebenice, Prosetín, and Muckov localities. It is abundant at Bližná, where in a reaction zone between the metacarbonate and the pegmatite is up to 10 cm thick zone containing axinite in addition to tourmaline (Novák et al., 1999).

Based on observed textural relations (Section 4.1) we suggest that in the samples with accessory tourmaline of paragenetic types I and II, the boron was internally derived because there is no evidence for strong interaction with the host rocks. In contrast, it is likely that external sources of boron were involved in forming tourmaline at the contact of marble with host silicate rock (paragenetic type III), in cross-cutting veins (type IV) and in the contact zone with the Bližná pegmatite (type V). This has implications for interpreting the B-isotope variations.

5.2. *The B-isotope variations in the context of the eastern Bohemian Massif*

Our data show that there are significant differences in the B-isotope ranges of accessory tourmaline in the different lithologic units of the

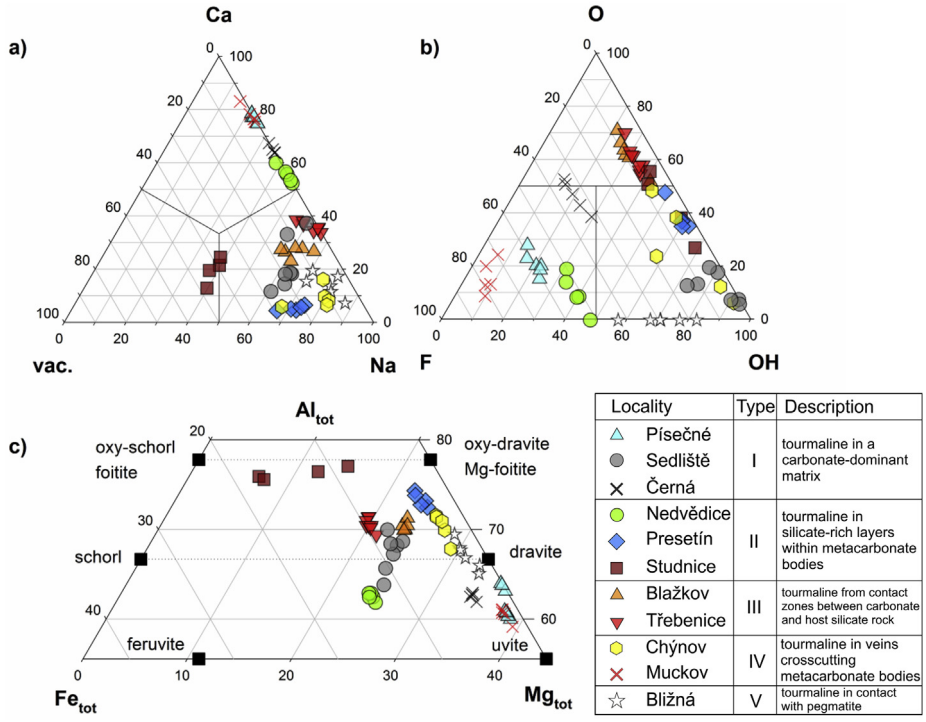

Fig. 4. Composition of tourmaline from studied metacarbonates and associated calc-silicate rocks from the investigated areas in the Bohemian Massif: (a) X-site; (b) W-site; (c) Y + Z sites.

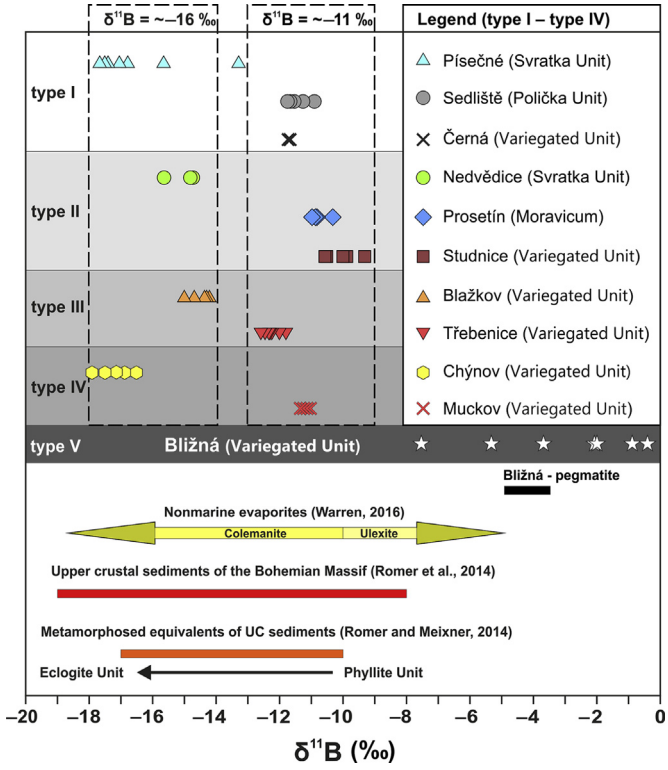

Fig. 5. Boron isotopic variations in tourmaline from metacarbonates and associated calc-silicate rocks from five paragenetic types (see text). Various geological units from the eastern part of Bohemian Massif given on right. The δ^{11}B values in tourmaline from axinite-bearing Bližná pegmatite (unpublished data of M. Novák) and other data for comparison: nonmarine evaporites (Warren, 2016), Gondwana-derived upper crustal sediments of the Bohemian Massif (Romer et al., 2014) and variously metamorphosed equivalents (Romer and Maixner, 2014).

Moldanubian Zone (Table 4). Samples from the Svratka Unit have a relatively light range of $\delta^{11}B_{tourmaline}$ (−18‰ to −14‰), whereas tourmaline from metacarbonates in adjacent Polička and Olešnice units has exclusively heavier δ^{11}B ranges (−13‰ to −9‰). In contrast, the Variegated Unit hosts metacarbonates containing tourmaline with both ranges of B-isotope ratios.

Generally, observed B isotope signatures largely overlap with the range of B isotopic composition reported for crystalline rocks of the continental crust (Trumbull and Slack, 2018 and references therein). The variations from paragenetic types I–IV over a range of ~8 δ-units is similar to the change in B isotopic composition of metapelitic rocks from the Bohemian Massif from different metamorphic grades (very-low grade to eclogite facies; Romer and Maixner, 2014; Fig. 5).

In the absence of tourmaline to buffer the isotope composition, prograde metamorphism involving dehydration reaction tends to produce minerals with decreasing δ^{11}B because ^{11}B is partitioned into the fluid phase (e.g., Trumbull and Slack, 2018). The range observed in the metacarbonate units, and the difference between relatively light (Svratka) and heavier (Polička and Olešnice) boron could reflect this effect. Magmatic boron can also play a role in the δ^{11}B signature of tourmaline. There are tourmaline-bearing granites and granitic pegmatites in the eastern part of the Bohemian Massif. The isotopic composition of those rocks is not well documented but the available studies, together with whole-rock B isotope signature of mantle-derived lamprophyric/lamproitic rocks of the Bohemian Massif (unpublished SIMS and TIMS data; Marschall and Ludwig, 2006; Míková et al., 2010) suggest an overlapping in δ^{11}B signature with the range of B isotope ratios in tourmalines from the investigated metacarbonates.

5.3. Possible sources of B

5.3.1. Nonmarine evaporites

The observed variations from –9‰ to –18‰ $\delta^{11}B_{tourmaline}$ corresponds with variations in nonmarine evaporite sequences (Fig. 5). This range can be explained by variable proportions of the borate minerals colemanite and ulexite (Warren, 2016 and references therein). However, the mineral

assemblages of the metacarbonates and their rock associations do not directly confirm that there were evaporites in the protolith. The exception to this is the locality Prosetín, where tourmaline occurs in association with albite and scapolite. If one accepts the idea that the light B-isotope signature is due to evaporites, this has implications for specific paleogeographic and climatic conditions during the early Palaeozoic. The arid conditions with isolated basins in a terrestrial landscape needed for the formation of nonmarine brines are at least plausible in the Moravo-Silesian Zone (locality Prosetín), where thick sedimentary sequences of Lower Palaeozoic "Old Red" terrestrial clastic material were deposited (e.g., Timmerman et al., 2018b and references therein). However, we caution that the involvement of evaporites is allowed by the B-isotope data but not required to explain the observed δ^{11}B values so it remains speculative.

5.3.2. Muscovite-bearing host rocks

It is well known that clay minerals and micas effectively concentrate ^{10}B due to the tetrahedral coordination of boron in the sheet structure (e.g., Jung and Schreyer, 2002; Wunder et al., 2005 and references therein). Typical boron concentrations in white mica are in the hundreds of ppm, which makes this mineral the second-most important boron host in most crustal rocks after tourmaline. Thus, clay- and mica-rich protoliths will be expected to have relatively light B-isotope signatures. Prograde metamorphism of metapelites will produce progressively lighter B-isotope compositions in the rocks since the metamorphic fluid released by dehydration is enriched in ^{11}B relative to the residual mineral phases (e.g., Romer and Maixner, 2014). As a result, the observed B isotope variants can be achieved, at least in the paragenetic metacarbonate types with heavier $\delta^{11}B_{tourmaline}$ signature (cf. Jung and Schreyer, 2002). This is in line with the data from the locality Muckov, where the abundance of muscovite in the host rock is low and the associated marble contains only scarce paragenetic type IV tourmaline which has relatively heavy and uniform B isotope composition (cf. Tables 1 and 4, Fig. 5). Also, type IV tourmaline in veins at the locality Chýnov (Fig. 2e) suggests an input of hydrous, boron-bearing fluids from an external source.

The low degree of variability on individual localities in B isotope composition (~1 δ-unit) suggests relatively uniform temperature conditions during tourmaline crystallisation. This is in line with estimated (p)-T conditions of 500–600 °C based on the observed mineral paragenesis (Houzar et al., 2017). The exception is observed at the locality Písečné, where tourmaline displays an "altered" zone, which is ~4 δ-units lighter in B isotope composition compared to other parts. Given a constant fluid composition, the isotope shift in late tourmaline from "altered" zone might be explained by a lower temperature. The fractionation factors of Meyer et al. (2008) imply a fluid-tourmaline fractionation of 1.3‰ at 600 °C and 5.4‰ at 150 °C. Alternatively, the fractures may have been infiltrated by a different fluid with a lower δ^{11}B composition.

5.3.3. Magmatic boron

Tourmaline from the pegmatite exocontact of paragenetic type V differs significantly from tourmaline in all other paragenetic types by its distinctively heavier δ^{11}B signature ranging from –7.7‰ to 0.6‰. This composition is not typical for boron isotope ratios in pegmatitic tourmalines, which are generally less than –10‰ (e.g., Marschall and Ludwig, 2006; Trumbull and Slack, 2018). The heavy B isotope signature may be explained by its occurrence in the exocontact of a Li pegmatite with abundant axinite. Because ^{10}B is preferably incorporated into axinite (e.g., Martin et al., 2016), the exocontact fluid would have a substantial depletion in ^{10}B, resulting in tourmaline with a heavy δ^{11}B signature, as observed in the marble and the associated pegmatite (see Fig. 5). Alternatively, heavy δ^{11}B signature could be a primary feature of magmatic fluids associated with this exotic pegmatite.

6. Conclusions

From this boron isotope study of tourmaline from metacarbonates and associated calc-silicate rocks of the eastern part of Bohemian Massif Bohemian Massif we make the following conclusions:

(1) Tourmaline-bearing metacarbonates and associated calc-silicate rocks (usually <50 m thick) are abundant in the Variegated Unit of the Moldanubian Zone and in the adjacent metamorphic complexes that are genetically linked to the Kutná Hora-Svratka Complex (Moldanubian Zone s.l.), Teplá–Barrandian or Moravo-Silesian zones.
(2) Five principal tourmaline occurrences were recognized in metacarbonate/calc-silicate bodies. Individual paragenetic types have distinctive compositional features. Fluor-uvite > dravite >> magnesio-lucchesiite are typical for the type I (marble-hosted tourmaline), whereas tourmalines from the type II (silicates-rich layers/nests), and type III (contact zones) are more variable, with oxy-schorl to magnesio-foitite, Al-rich dravite, fluor-uvite in type II and Ca,Ti-bearing oxy-dravite in type III, respectively. The type IV (veins) feature dravite and fluor-uvite compositions, whereas the type V (pegmatite exocontact) contains Li,F-rich dravite.
(3) Where tourmaline is the only B-bearing phase (paragenetic types I–IV) it is characterized by two principal δ^{11}B signatures (δ^{11}B = ~–11‰ and ~–16‰), which largely overlap with the range of isotopic compositions reported for crystalline rocks of the continental crust. An exception is paragenetic type V (elbaite-subtype pegmatite Bližná; Moldanubian Zone) with δ^{11}B of –7‰ to 0.6‰. In this case, the presence of cogenetic axinite depletes the residual melt and/or fluids in ^{10}B, causing a shift of tourmaline towards heavier values.
(4) The Variegated Unit of the Moldanubian Zone hosts metacarbonates containing tourmaline with both the heavy and light B-isotope signatures. The Svratka Unit (Moldanubian Zone s.l.) hosts only isotopically lighter δ^{11}B tourmaline, whereas tourmaline from metacarbonates in adjacent Polička unit (Teplá–Barrandian Zone) and Olešnice unit (Moravicum of the Moravo-Silesian Zone) displays only isotopically heavier δ^{11}B signatures.
(5) The relatively light B isotope signature of tourmaline may be indicative for boron sourced from continental (non-marine) evaporites. However, the observed range of ~8 δ-units is also consistent with the change in B isotopic composition of metasedimentary rocks of the Bohemian Massif which is attributed to prograde metamorphism from very-low grade to eclogite facies. A magmatic source of boron may also be considered because the B-isotope ratios of tourmaline from granites and granitic pegmatites in the Moldanubian Zone and adjacent metamorphic complexes of the Bohemian Massif, as well as lamprophyric/lamproitic intrusions derived from crust-metasomatised lithospheric mantle overlap with the range of B isotope ratios in tourmaline from the metacarbonates. This study indicates the complexity of processes influencing the B isotope signatures, both in the regional context of boron cycling during prograde metamorphosis, and in the local context of partitioning with coexisting B-compatible minerals (e.g., muscovite, axinite).

Declaration of competing interest

The authors declare that they have no known competing financial interests or personal relationships that could have appeared to influence the work reported in this paper.

Acknowledgments

This work was financially supported by the research project of the Czech Science Foundation (GAČR 17-17276S) "Tourmaline – an indicator of geological processes". The work of LK was also supported by the institutional project RVO 67985831 of the Institute of Geology of the Czech Academy of Sciences, as well as by the Brno University of

Technology project LO1408 "AdMaS UP – Advanced Materials, Structures and Technologies", supported by the Ministry of Education, Youth and Sports CR under the "National Sustainability Programme I". The work of SH was covered through financial support provided to the Moravian Museum by the Ministry of Culture of the Czech Republic as part of its long-term conceptual development programme for research institutions (ref. MK000094862) (S.H.). We thank J. Cícha and J. Zikeš for the tourmaline samples from Muckov and Černá. The authors greatly appreciate Barbara Dutrow (Louisiana State University) and Vincent van Hinsberg (McGill University) for their very constructive and helpful comments and suggestions and Kristoffer Szilas for excellent editorial handling.

Appendix A. Supplementary data

Supplementary data to this article can be found online at https://doi.org/10.1016/j.gsf.2020.03.009.

References

Bačík, P., Cempírek, J., Uher, P., Novák, M., Ozdín, D., Škoda, R., Breiter, K., Klementová, M., Ďuďa, R., Groat A., L., 2013. Oxy-schorl, $Na(Fe_2^{2+}Al)Al_6Si_6O_{18}(BO_3)_3(OH)_3O$, a new mineral from Zlatá Idka, Slovak Republic and Přibyslavice, Czech Republic. Am. Mineral. 98, 485–492.

Bačík, P., Uher, P., Cempírek, J., Vaculovič, T., 2012. Magnesian tourmalines from plagioclase-muscovite-scapolite metaevaporite layers in dolomite marble near Prosetín (Olešnice Unit, Moravicum, Czech Republic). J. Geosci. 57, 143–153.

Buriánek, D., Novák, M., 2007. Compositional evolution and substitutions in disseminated and nodular tourmaline from leucocratic granites: examples from the Bohemian Massif, Czech Republic. Lithos 95, 148–164.

Buriánek, D., Novák, M., Cempírek, J., 2017. Geological background. In: Gadas, P., Novák, M. (Eds.), Tourmalines of the Eastern Part of the Bohemian Massif. Tigris, Zlín, pp. 3–10.

Buriánek, D., Verner, K., Hanžl, P., Krumlová, H., 2009. Ordovician metagranites and migmatites of the Svratka and Orlice-Sněžník units, northeastern Bohemian massif. J. Geosci. 54, 181–200.

Catanzaro, E.J., Champion, C.E., Garner, E.L., Maienko, G., Sappenfield, K.M., Shields, W.R., 1970. Standard Reference Materials: Boric Acid; Isotopic, and Assay Standard Reference Materials. National Bureau of Standards, Washington, D.C., p. 62

Čopjaková, R., Buriánek, D., Škoda, R., Houzar, S., 2009. Tourmalinites in the metamorphic complex of the Svratka Unit (Bohemian Massif): a study of compositional growth of tourmaline and genetic relations. J. Geosci. 54, 221–243.

Deer, W.A., Howie, R.A., Zussman, J., 1997. Rock-Forming Minerals: Disilicates and Ring Silicates, second ed., 1B. Geological Society of London, London, p. 629.

Dutrow, B.L., Henry, D.J., 2011. Tourmaline: a geologic DVD. Elements 7, 301–306.

Dyar, M.D., Taylor, M.E., Lutz, T.M., Francis, C.A., Guidotti, C.V., Wise, M., 1998. Inclusive chemical characterization of tourmaline: Mössbauer study of Fe valence and site occupancy. Am. Mineral. 83, 848–864.

Dyar, M.D., Wiedenbeck, M., Robertson, D., Cross, L.R., Delaney, J.S., Ferguson, K.M., Francis, C.A., Grew, E.S., Guidotti, C.V., Hervig, R.L., Hughes, J.M., Husler, J., Leeman, W., McGuire, A.V., Rhede, D., Rothe, H., Paul, R.L., Richards, I., Yates, M., 2001. Reference minerals for microanalysis of light elements. Geostand. Newsl. 25, 441–463.

Finger, F., Gerdes, A., Janoušek, V., René, M., Riegler, G., 2007. Resolving the Variscan evolution of the Moldanubian sector of the Bohemian massif: the significance of the Bavarian and the Moravo–Moldanubian tectonometamorphic phases. J. Geosci. 52, 9–28.

Gadas, P., Novák, M., Staněk, J., Filip, J., Vašinová Galiová, M., 2012. Compositional evolution of zoned tourmaline crystals from pockets in common pegmatites, the Moldanubian Zone, Czech Republic. Can. Mineral. 50, 895–912.

Grice, J.D., Ercit, T.S., 1993. Ordering of Fe and Mg in the tourmaline crystal structure: correct formula. Neues Jahrbuch Mineral. Abhand. 165, 245–266.

Groat, L.A., Evans, R.J., Cempírek, J., McCammon, C., Houzar, S., 2013. Fe-rich and As-bearing vesuvian and wiluite from Kozlov, Czech Republic. Am. Mineral. 98, 1330–1337.

Guy, A., Edel, J.B., Schulmann, K., Tomek, Č., Lexa, O., 2011. A geophysical model of the Variscan orogenic root (Bohemian Massif): implications for modern collisional orogens. Lithos 124, 144–157.

Henry, D., Novák, M., Hawthorne C., F., Ertl, A., Dutrow, B., Uher, P., Pezzotta, F., 2011. Nomenclature of the tourmaline-group minerals. Am. Mineral. 96, 895–913.

Houzar, S., Doležalová, H., Novák, M., Hrazdil, V., Přeiferová, A., 2006. Mineralogy, petrography and geology of the Nedvědice marbles, Svratka crystalline complex; a review. Acta Musei Morav. Sci. Geol. 91, 3–77.

Houzar, S., Novák, M., Cícha, J., 2017. Mineral assemblages and lithology of marbles of the Bohemian part of the Moldanubian zone (Bohemian massif). Bull. Mineral. Petrol. 25, 113–140.

Jung, I., Schreyer, W., 2002. Synthesis, properties and stability of end member boromuscovite, $KAl_2[BSi_3O_{10}](OH)_2$. Contrib. Mineral. Petrol. 143, 684–693.

Kalvoda, J., Bábek, O., Fatka, O., Leichmann, J., Melichar, R., Nehyba, S., Špaček, P., 2008. Brunovistulian terrane (Bohemian massif, central Europe) from late Proterozoic to late Paleozoic: a review. Int. J. Earth Sci. 97, 497–518.

Kossmat, F., 1927. Gliederung des varistischen Gebirgsbaues. Abhandlungen des Sächsischen Geologischen Landesamtes 1, pp. 1–39 (in German).

Kříbek, B., 1997. Carbonaceous Formation of Bohemian Massif and Their Mineralization, first ed. Czech Geological Survey, Prague, p. 126.

Krmíček, L., Romer, R.L., Ulrych, J., Glodny, J., Prelević, D., 2016. Petrogenesis of orogenic lamproites of the Bohemian Massif: Sr–Nd–Pb–Li isotope constraints for Variscan enrichment of ultra-depleted mantle domains. Gondwana Res. 35, 198–216.

Kroner, U., Romer, R.L., 2013. Two plates – many subduction zones: the Variscan orogeny reconsidered. Gondwana Res. 24, 298–329.

Malecha, A., Suk, M., Vachtl, J., 1960. Geology and petrology of crystalline complex between Sušice and Horaždovice. Sborník Ústředního ústavu geologického, Oddělení geologie 26, 531–583.

Marschall, H.R., Ludwig, T., 2006. Re-examination of the boron isotopic composition of tourmaline from the Lavicky granite, Czech Republic, by secondary ion mass spectrometry: back to normal. Geochem. J. 40, 631–638.

Marschall, H.R., Jiang, S.Y., 2011. Tourmaline isotopes: no element left behind. Elements 7 (5), 313–319.

Martin, C., Flores E., K., Harlow E., G., 2016. Boron isotopic discrimination for subduction-related serpentinites. Geology 44, 899–902.

Matte, P., Maluski, H., Rajlich, P., Franke, W., 1990. Terrane boundaries in the Bohemian Massif: result of large-scale Variscan shearing. Tectonophysics 177, 151–170.

McCann, T., 2008. In: The geology of Central Europe. Volume I: Precambrian and Palaeozoic. Geological Society of London, London, pp. 1–748.

Meyer, C., Wunder, B., Meixner, A., Romer L., R., Heinrich, W., 2008. Boron-isotope fractionation between tourmaline and fluid: an experimental re-investigation. Contributions to Mineralogy and Petrology 156, 259–267.

Míková, J., Novák, M., Janoušek, V., 2010. Boron isotopes in tourmaline of dravite–schorl series from granitic pegmatites of the Moldanubian Zone, Czech Republic. Acta Minerol.-Petrogr. (Szeged) 6, 475.

Novák, M., 1989. Metamorphism of dolomitic rocks at the north-eastern margin of the Moldanubicum, Western Moravia, Czechoslovakia. Acta Musei Moraviae, Scientiae naturales 74, 7–51 (in Czech with English abstract).

Novák, M., Filip, J., Selway, J.B., 2003. Locality No. 1 Sedliště near Polička, calcite marble. In: Novák, M. (Ed.), Field Trip Guidebook – LERM 2003. Masaryk University, Brno, pp. 11–16.

Novák, M., Selway, J.B., Černý, P., Hawthorne, F.C., 1999. Tourmaline of the elbaite-dravite series from an elbaite-subtype pegmatite at Bližná, southern Bohemia, Czech Republic. Eur. J. Mineral 11, 557–568.

Novák, M., Škoda, R., Filip, J., Macek, I., Vaculovič, T., 2011. Compositional trends in tourmaline from intragranitic NYF pegmatites of the Třebíč Pluton, Czech Republic: an electron microprobe, Mössbauer and LA–ICP–MS study. Can. Mineral. 49, 359–380.

Novák, M., Škoda, R., Gadas, P., Krmíček, L., Černý, P., 2012. Contrasting origins of the mixed (NYF + LCT) signature in granitic pegmatites, with examples from the Moldanubian Zone, Czech Republic. Can. Mineral. 50, 1077–1094.

Povondra, P., Novák, M., 1986. Tourmalines from metamorphosed carbonate rocks from western Moravia. Neues Jahrbuch Mineral. Monatsh. 6, 273–282.

Romer, R.L., Maixner, A., 2014. Lithium and boron isotopic fractionation in sedimentary rocks during metamorphism – the role of rock composition and protolith mineralogy. Geochem. Cosmochim. Acta 128, 158–177.

Schulmann, K., Lexa, O., Janoušek, V., Lardeaux, J.M., Edel, J.B., 2014. Anatomy of a diffuse cryptic suture zone: an example from the Bohemian Massif, European Variscides. Geology 42, 275–278.

Selway B., J., Novák, M., Černý, P., Hawthorne C., F., 1999. Compositional evolution of tourmaline in lepidolite-subtype pegmatites. Eur. J. Mineral. 11, 569–584.

Slobodník, M., Hladíková, J., 1994. Sulphidic mineralization in the Polička crystalline complex; a discussion of the sediment-hosted type mineralization. Bull. Geol. Surv. 69, 37–45.

Stephan, T., Kroner, U., Romer, R.L., Rösel, D., 2019. From a bipartite Gondwana shelf to an arcuate Variscan belt: the early Paleozoic evolution of northern Peri-Gondwana. Earth Sci. Rev. 192, 491–512.

Suess, F.E., 1926. Intrusionstektonik und Wandertektonik im variszischen Grundgebirge. Gebrüder Borntraeger, Berlin, p. 268 (in German).

Timmerman, M.J., Krmíček, L., Kubouśková, S., Sláma, J., Sobel, E., 2018a. LA-ICP-MS U–Pb zircon dating of plutonic and metavolcanic rocks of Slavkov Terrane and Central Basic Belt, Brunovistulian microcontinent – preliminary results. In: Kubouśková, S., Krmíček, L. (Eds.), Proceedings of the Brunovistulicum 2018 Conference. Masaryk University, Brno, pp. 4–15.

Timmerman, M.J., Krmíček, L., Kubouśková, S., Sláma, J., Sobel, E., 2018b. LA-ICP-MS U–Pb zircon provenance of the Lower Palaeozoic "basal clastics" sediment cover of the Slavkov Terrane, Brunovistulian microcontinent – preliminary results. In: Kubouśková, S., Krmíček, L. (Eds.), Proceedings of the Brunovistulicum 2018 Conference. Masaryk University, Brno, pp. 19–28.

Trumbull, R.B., Slack, J.F., 2018. Boron isotopes in the continental crust: granites, pegmatites, felsic volcanic rocks and related ore deposits. In: Marschall, H.R., Foster, G.L. (Eds.), Boron Isotopes – the Fifth Element, Advances in Geochemistry, vol. 7. Springer, Heidelberg, pp. 249–272.

van Hinsberg, V.J., Henry, D.J., Marschall, H.R., 2011. Tourmaline: an ideal indicator of its host environment. Can. Mineral. 49, 1–16.

Vrána, S., 1997. Locality No. 9: Hluboká nad Vltavou; tourmaline-bearing alkali-feldspar orthogneiss. In: Novák, M., Selway, J.B. (Eds.), "Tourmaline 1997": International Symposium on Tourmaline: June 20 to 25, 1997. Czech Geological Survey, Prague, pp. 99–104.

Vrána, S., Novák, M., Selway, J.B., 1997. Locality No. 8: Chýnov near Tábor; mica-rich rock with Cr-bearing muscovite and accessory Cr-bearing dravite, dravite veinlets in dolomite. In: Novák, M., Selway, J.B. (Eds.), "Tourmaline 1997": International Symposium on Tourmaline: June 20 to 25, 1997. Czech Geological Survey, Prague, pp. 95–98.
Warren, J.K., 2016. Evaporites: A Geological Compendium. Springer, Cham, p. 1813.
Whitney, D.L., Evans, B.W., 2010. Abbreviations for names of rock-forming minerals. Am. Mineral. 95, 185–187.
Wunder, B., Meixner, A., Romer, R.L., Wirth, R., Heinrich, W., 2005. The geochemical cycle of boron: constraints from boron isotope partitioning experiments between mica and fluid. Lithos 84, 206–216.
Žák, J., Sláma, J., 2018. How far did the Cadomian 'terranes' travel from Gondwana during early Palaeozoic? A critical reappraisal based on detrital zircon geochronology. Int. Geol. Rev. 60, 319–338.